

Calibration Comparison Method for Vector Network Analyzers

Roger B. Marks, Jeffrey A. Jargon, and John R. Juroshek

National Institute of Standards and Technology
325 Broadway, Mail Code 813.06, Boulder, CO 80303 USA
Tel: (303)497-3037 Fax: (303)497-3970
E-mail: marks@nist.gov

ABSTRACT

We present a technique for comparing the scattering parameter measurements made with respect to two vector network analyzer calibrations. This method determines the worst-case measurement error bounds on any calibration from a benchmark calibration, assuming the two are similar to first order. We illustrate our method by examining the differences between an open-short-load-thru (OSLT) and a sliding load calibration, both of which are available commercially on a variety of vector network analyzers.

INTRODUCTION

In this paper, we develop the ability to quantify the difference between scattering parameter (S-parameter) measurements made with respect to any two vector network analyzer (VNA) calibrations. Our model assumes that the switching and isolation errors in the VNA are either negligible or have been correctly accounted for. Then, assuming that the two calibrations in question are similar to first order, we determine worst-case deviations between the measured S-parameters.

Certain methods of calibration, such as multiline thru-reflect-line (TRL) [1], provide high accuracy, while others are less time consuming and make use of simple standard artifacts. Thus, many users may wish to obtain detailed error bounds on a simpler calibration with respect to a benchmark calibration of known accuracy. The ability to compare calibrations can give them a quantitative way to help determine if a more convenient calibration scheme will meet their accuracy needs.

Williams and Marks [2] recently developed a technique for comparing calibrations. In summary, their method makes use of a benchmark two-tier multiline TRL calibration performed with respect to an initial calibration whose accuracy is of interest. This procedure has proven useful in a number of situations, including the verification of probe-tip calibrations [3,4] and line-reflect-match calibrations [5,6]. The only difficulty with this comparison is that a two-tier calibration scheme is required. Since most VNAs do not usually come equipped with this capability, external calibration software is required to obtain the desired error bounds. Oftentimes, however, users are interested in comparing two commercially available calibration schemes.

CALIBRATION COMPARISON

A two-port VNA, shown in Fig. 1, in which the switching and isolation errors are either negligible or have been correctly accounted for, provides a measurement M_i of the product of three matrices:

$$M_i = XT_i\bar{Y}, \quad (1)$$

where T_i is the cascade matrix of the device i under test, X and Y are constant, nonsingular matrices which describe the instrument, and

$$\bar{Y} \equiv \tilde{Y}^{-1} \equiv \begin{bmatrix} 0 & 1 \\ 1 & 0 \end{bmatrix} Y^{-1} \begin{bmatrix} 0 & 1 \\ 1 & 0 \end{bmatrix} \quad (2)$$

is the reverse cascade matrix corresponding to Y [7]. The calibration requires connecting a number of standards whose cascade matrices T_i are assumed to be known. When

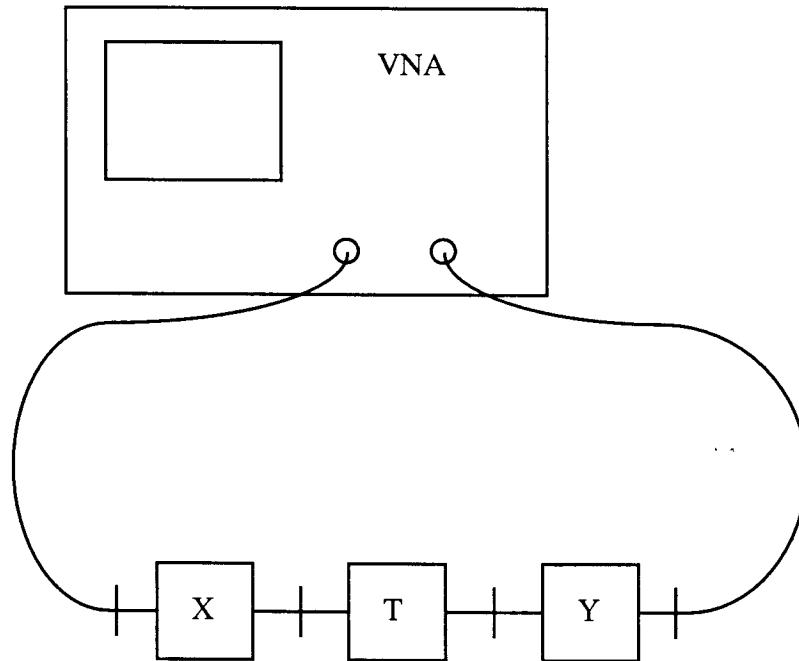


Figure 1. A two-port vector network analyzer provides a measurement of the product of three matrices, where T is the cascade matrix of the device under test, and X and Y are matrices which describe the instrument.

enough measurements M_i are available, the matrices X^M and Y^M are determined, and the cascade matrix T^M of a device is calculated from the uncorrected measurement M by

$$T^M = (X^M)^{-1} M (\overline{Y^M})^{-1}. \quad (3)$$

Assuming a 12-term error model, X^M and Y^M may be computed from the calibration coefficients. One possible formulation is

$$X^M = \begin{bmatrix} E_{RF} - E_{DF}E_{SF} & E_{DF} \\ -E_{SF} & 1 \end{bmatrix} \quad (4)$$

and

$$Y^M = \frac{E_{TF}(1 - E_{DR}\Gamma_2)}{E_{RR}} \begin{bmatrix} E_{RR} - E_{DR}E_{SR} & E_{DR} \\ -E_{SR} & 1 \end{bmatrix}, \quad (5)$$

where

$$\Gamma_2 = \frac{E_{LF} - E_{SR}}{E_{RR} + E_{DR}(E_{LF} - E_{SR})}. \quad (6)$$

The calibration coefficients are illustrated in Fig. 2.

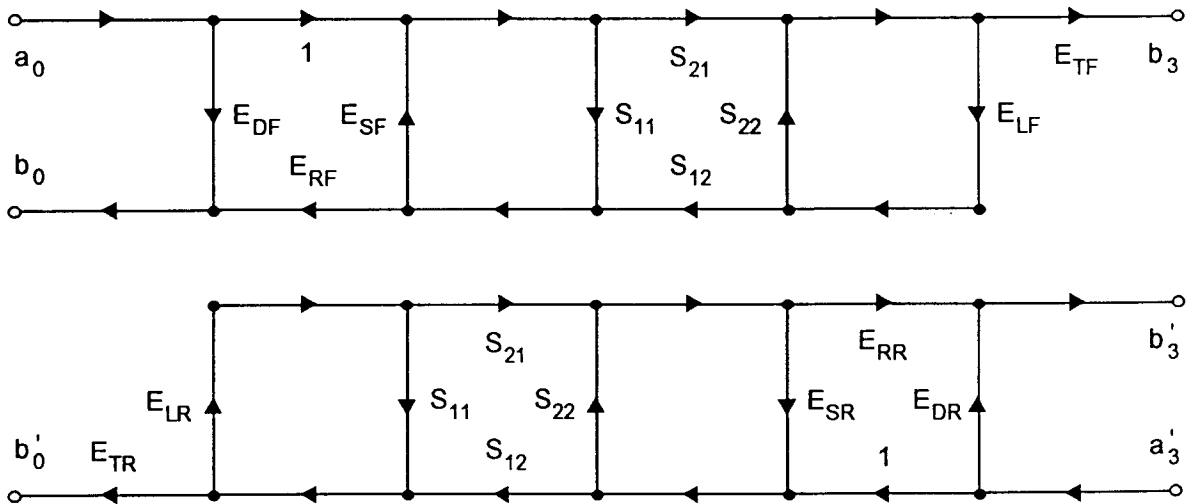


Figure 2. Conventional network analyzer error model. S is the device under test. The top diagram applies when power is applied to Port 1, the bottom for power on Port 2. The isolation terms are omitted from this diagram.

If a second calibration N is performed, the cascade matrix T^N calculated for the same device is given by

$$T^N = (X^N)^{-1} M (\overline{Y^N})^{-1}. \quad (7)$$

Combining eqs. (3) and (7) leads to

$$T^M = [(X^M)^{-1} X^N] T^N [\overline{Y^N} (\overline{Y^M})^{-1}] \equiv X T^N \overline{Y}. \quad (8)$$

The matrices X and Y are independent of the device under test and describe the differences between measurements performed with respect to the two calibrations. If the calibrations are identical, then $T^M = T^N$, and X and Y are each equal to the identity matrix I . If the calibrations differ, however, then

$$T^M = (I + \delta^X) T^N (\overline{I + \delta^Y}), \quad (9)$$

where

$$\delta^X = X - I ; \quad \delta^Y = Y - I \quad (10)$$

are deviations from the identity matrix.

With this model, we would like to determine worst-case deviations between the measured S-parameters S_{ij}^M , which correspond to the cascade matrix T^M measured by calibration M , and the S-parameters S_{ij}^N , which correspond to the cascade matrix T^N measured by calibration N . If $|\delta_{ij}^Y| \ll 1$, the inverse cascade matrix of $I + \delta^Y$ is approximated by

$$\overline{(I + \delta^Y)} = \widetilde{(I + \delta^Y)^{-1}} \approx \widetilde{(I - \delta^Y)} = I - \widetilde{\delta^Y} \quad (11)$$

if we keep only the terms which are linear in δ_{ij}^Y . If $|\delta_{ij}^X| \ll 1$ as well, T^M is approximated by

$$T^M \approx (I + \delta^X) T^N (I - \widetilde{\delta^Y}) \approx T^N + T^N \delta^X - T^N \widetilde{\delta^Y}. \quad (12)$$

The expression for S_{21}^M in terms of T^M is

$$S_{21}^M = \frac{1}{T_{22}^M} \approx \frac{1}{T_{22} (1 + \delta_{22}^X + \delta_{21}^X T_{12}/T_{22} - \delta_{11}^Y - \delta_{21}^Y T_{21}/T_{22})}. \quad (13)$$

To linear order,

$$S_{21}^M \approx S_{21} (1 - \delta_{22}^X + \delta_{11}^Y - \delta_{21}^Y S_{22} - \delta_{21}^X S_{11}). \quad (14)$$

which implies

$$\frac{|S_{21}^M - S_{21}|}{|S_{21}|} \leq |\delta_{11}^Y - \delta_{22}^X| + |S_{22}| |\delta_{21}^Y| + |S_{11}| |\delta_{21}^X|. \quad (15)$$

We use the \leq to indicate the inequality is valid only when $|\delta_{ij}^X| \ll 1$ and $|\delta_{ij}^Y| \ll 1$. The same procedure is used to obtain the bounds

$$\frac{|S_{12}^M - S_{12}|}{|S_{12}|} \leq |\delta_{11}^X - \delta_{22}^Y| + |S_{22}| |\delta_{21}^Y| + |S_{11}| |\delta_{21}^X|, \quad (16)$$

$$|S_{11}^M - S_{11}| \leq |\delta_{12}^X| + |S_{11}| |\delta_{11}^X - \delta_{22}^X| + |S_{21} S_{12}| |\delta_{21}^Y| + |S_{11}|^2 |\delta_{21}^X|, \quad (17)$$

and

$$|S_{22}^M - S_{22}| \leq |\delta_{12}^Y| + |S_{22}| |\delta_{11}^Y - \delta_{22}^Y| + |S_{21} S_{12}| |\delta_{21}^X| + |S_{22}|^2 |\delta_{21}^Y|. \quad (18)$$

If the S_{ij} are known, then these expressions give bounds for $|S_{ij}^M - S_{ij}|$. Whenever $\max |S_{ij}| \leq 1$, which is satisfied by passive devices when the reference impedance of calibration N is real at each port,

$$|S_{11}^M - S_{11}| \leq \epsilon_{11} \equiv |\delta_{11}^X - \delta_{22}^X| + |\delta_{21}^X| + |\delta_{12}^X| + |\delta_{21}^Y|, \quad (19)$$

$$\frac{|S_{21}^M - S_{21}|}{|S_{21}|} \leq \epsilon_{21} \equiv |\delta_{11}^Y - \delta_{22}^X| + |\delta_{21}^X| + |\delta_{21}^Y|, \quad (20)$$

$$\frac{|S_{12}^M - S_{12}|}{|S_{12}|} \leq \epsilon_{12} \equiv |\delta_{11}^X - \delta_{22}^Y| + |\delta_{21}^Y| + |\delta_{21}^X|, \quad (21)$$

$$|S_{22}^M - S_{22}| \leq \epsilon_{22} \equiv |\delta_{11}^Y - \delta_{22}^Y| + |\delta_{21}^Y| + |\delta_{12}^Y| + |\delta_{21}^X|, \quad (22)$$

and

$$|S_{ij}^M - S_{ij}| \leq \epsilon \equiv \max_{mn} (\epsilon_{mn}). \quad (23)$$

Note that these worst-case deviations are identical to those in the two-tier calibration comparison. The difference between the two methods is in how the values of δ are computed. In the two-tier case, they are determined by the second-tier calibration, which identifies the error boxes relating the two calibrations. In this case, the values of δ are calculated from the difference of two first-tier calibrations, as we have shown above.

ILLUSTRATION

To illustrate our technique, we compared an OSLT calibration to a sliding load calibration, both of which are available commercially on a variety of VNAs. The two calibrations were performed consecutively on a VNA using APC-7 connectors from 45 MHz to 18 GHz. Figures 3-4 illustrate the bounds on measured S-parameters for S_{11} and S_{21} . Three curves appear on each graph. The uppermost curve represents the calculated bounds between the sliding load and OSLT calibrations, the middle one represents differences between actual measurements of a device for the two calibrations, and the lowermost one shows the repeatability between two consecutive sliding load calibrations. For S_{21} we measured a 25 Ω mismatch airline, and for S_{11} we measured a 25 Ω mismatch airline terminated with an offset short. The 25 Ω mismatch airline was used to add extra reflection and phase change to the measurement. The calculated bounds do indeed bound the actual measurement differences at all frequencies.

In Figs. 3-4, the worst-case bounds between the two different calibrations suddenly increase in value at 2 GHz. The reason for this is that the VNA's built-in sliding load calibration requires a fixed load for measurements under 2 GHz due to the poor performance of the sliding load at low frequencies. In our case, we used the same load here as we did in the OSLT calibration. Thus, below 2 GHz, our error bound simply measures the difference between two "identical" OSLT calibrations.

CONCLUSIONS

We have shown a useful technique for verifying calibrations by computing worst-case measurement bounds on scattering parameter measurements. We illustrated this method by comparing two commercially available calibrations, and showed that the differences between measured devices were always bounded by our calculated values.

We have found that, in comparing calibrations, the isolation terms are often negligible. However, ignoring the switching errors can lead to inaccuracies [8].

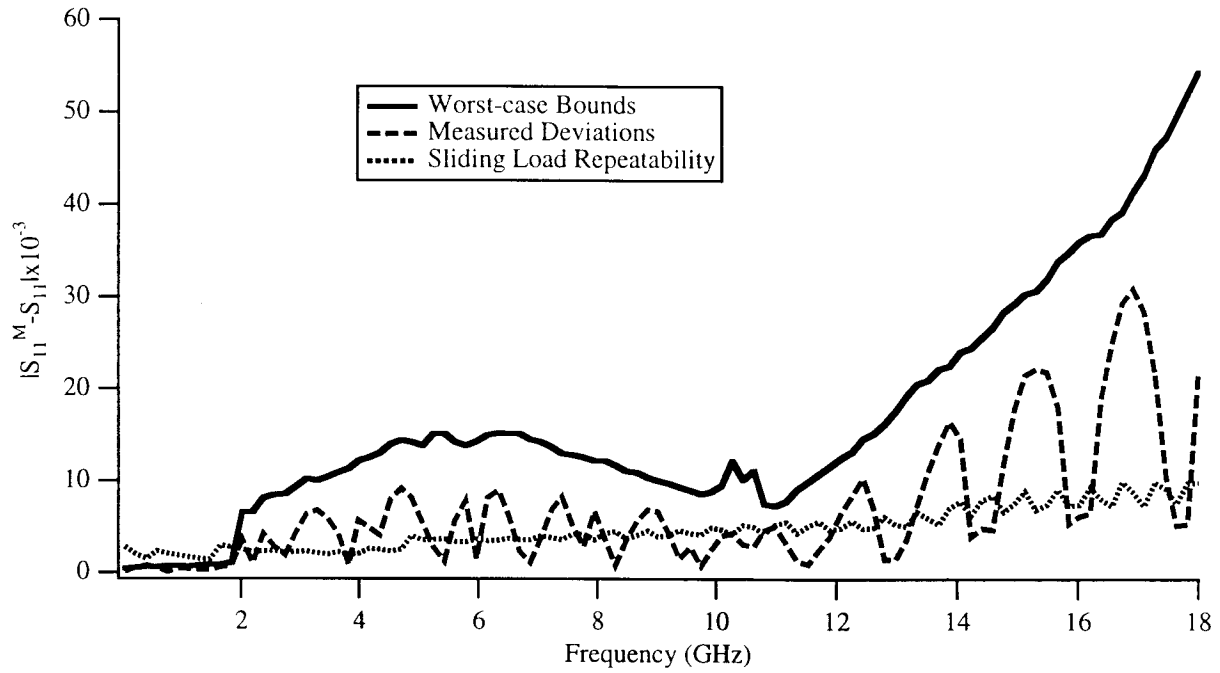


Figure 3. Worst-case error bounds and measured deviations for S_{11} between an OSLT calibration and a sliding load calibration.

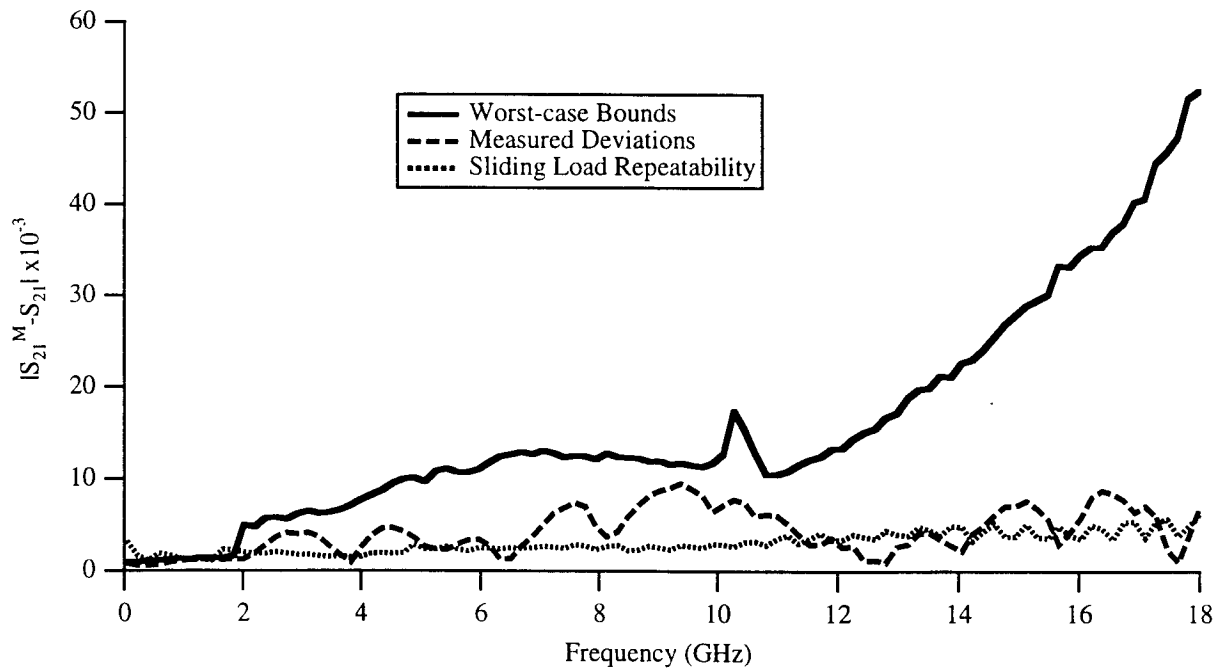


Figure 4. Worst-case error bounds and measured deviations for S_{21} between an OSLT calibration and a sliding load calibration.

ACKNOWLEDGMENTS

We thank Michael Janezic for his assistance with the measurements, and Larry Tarr and Michael McPartlin for reviewing this manuscript.

REFERENCES

- [1] R.B. Marks, "A Multiline Method of Network Analyzer Calibration," *IEEE Trans. Microwave Theory Tech.* Vol. 39, pp. 1205-1215, Jul. 1991.
- [2] D.F. Williams, R.B. Marks, and A. Davidson, "Comparison of On-Wafer Calibrations," *38th ARFTG Conf. Dig.*, pp. 68-81, Dec. 1991.
- [3] D.F. Williams and R.B. Marks, "Calibrating On-Wafer Probes to the Probe Tips," *40th ARFTG Conf. Dig.*, pp. 136-143, Dec. 1992.
- [4] R.B. Marks and D.F. Williams, "Verification of Commercial Probe-Tip Calibrations," *42nd ARFTG Conf. Dig.*, pp. 37-44, Dec. 1993.
- [5] D.F. Williams and R.B. Marks, "LRM Probe-Tip Calibrations with Imperfect Resistors and Lossy Lines," *42nd ARFTG Conf. Dig.*, pp. 32-36, Dec. 1993.
- [6] J.A. Jargon, R.B. Marks, and D.F. Williams, "Coaxial Line-Reflect-Match Calibration," *Asia-Pacific Microwave Conf. Proc.*, Vol.1, pp. 86-89, Oct. 1995.
- [7] R.B. Marks and D.F. Williams, "A General Waveguide Circuit Theory," *J. Res. Natl. Inst. Stand. Technol.*, Vol. 97, No. 5, pp. 533-562, Sep.-Oct. 1992.
- [8] J.A. Jargon and R.B. Marks, "Two-Tier Multiline TRL for Calibration of Low-Cost Network Analyzers," *46th ARFTG Conf. Dig.*, pp. 1-8, Nov.-Dec. 1995.